

# Quo Vadis Strangeness?

**Johann Rafelski**

Department of Physics, University of Arizona, Tucson, AZ 85721

**Abstract.** The study of strange and also charmed hadronic particle production in nuclear relativistic collisions offers an opportunity to explore the physical properties of the deconfined quark-gluon phase. We survey the recent accomplishments and the future directions of this research program.

## 1. Unde Venimus

### 1.1. Preamble

Nuclear collisions at relativistic energies are the experimental tool developed in the past 20 years to form, explore, and study a locally ‘color-melted’ space-time domain. At this time we are assembling comprehensive experimental evidence that a locally color deconfined state indeed is formed in present day experiments. I will present here my personal assessment of the recent developments, current status, and a view of near-future opportunities in searching for, and studying the quark-gluon plasma (QGP) using hadronic flavor observables, strangeness in particular. My deliberations and conclusions arise from reports and overviews presented at the Strangeness 1998 meeting [1].

The experimental and theoretical work of interest to us relies on the idea of strangeness enhancement. The ‘heavy’ quark flavor, which depending on the energy available in the relativistic nuclear collision can be strangeness or charm, is a fingerprint of the structure of dense matter created in two distinct ways:

- (i) the overall abundance has to be made nearly entirely during the early stages of the collision and thus this yield depends on the conditions early on;
- (ii) the flavor distribution in the hadronization process among different final state particles is able to populate otherwise rarely produced particles, such as strange antibaryons, which are most impacted by the onset of color-deconfinement.

The reach of our current research program centered at the SPS accelerator at CERN (European Center for Nuclear Research, Geneva area across French-Swiss border) and AGS accelerator at BNL (Brookhaven National Laboratory, Long Island, New York) will be extended within the next two years ten-fold in energy, with first data emerging from the Relativistic Heavy Ion Collider (RHIC), which is currently being completed at the BNL. By the year 2010 we will be able to explore entirely new horizons at CERN, where the Large Hadron Collider (LHC) will allow to create physical conditions rivaled only by the Big-Bang. This future time-line leads us through at least the period 2015–2020. Looking back to the early 1980’s when first

theoretical work has been published [2, 3, 4, 5, 6, 7], we see that in our work today we have at least as much future as there has been history.

There are yet other considerable research opportunities, as in the march towards higher energies, where the deconfinement is nearly a sure bet, we may have jumped the collision energy domain in which the effects related to critical behavior could be studied at the conditions that just suffice to melt the strongly interacting vacuum structure. At which energy this situation arises is presently still a hotly debated topic.

### 1.2. The principles

The physical ideas on which our research program depends are rather simple and hence dependable: if color deconfinement occurs, the quark-gluon soup will in due course equilibrate the flavor abundance between the light quarks  $u, d$ , that are brought into the collision and the initially absent heavier and on the laboratory time scale short lived  $s$  quarks. However, given the hadronic interaction scale of  $\tau_h c \simeq 10$  fm, the lifespan of strangeness,  $\tau_s c \simeq 10^{12} \tau_h$ , is of course infinite, as is the somewhat shorter lifespan of charm. Different mechanisms of flavor pair production have been explored and it is generally accepted that in the deconfined region heavy quarks are primarily produced in gluon fusion reactions [5, 8, 9]. For each  $s$ -quark made, there is its  $\bar{s}$  partner, since in strong interactions only quark pairs can be produced. The availability of an already prepared strange and anti-strange quark reservoir at QGP break-up allows quark clustering into multi-strange final state hadrons without ‘penalty’. In this way, the OZI rule is overcome. This collective effect, where key components of a final state particle are made in earlier reactions, is the source of our expectation that we can diagnose the presence of QGP using strongly interacting observables.

One of the keys to the understanding of the nature of dense matter provide gluons, the color charged cousins of photons. Gluons are the key distinction between the deconfined quark-gluon phase and the confined hadron gas. They are an important component in determining QGP properties, and they are the source of strangeness. Moreover, gluons play a major role in the dynamics of the QGP hadronization, since they carry much of the entropy that turns into particle abundance. The approximate gluon number density in QGP is given by:

$$\rho_g \simeq \left( \frac{T}{250 \text{ MeV}} \right)^3 \text{ fm}^{-3}. \quad (1)$$

Because gluons can be created and annihilated easily in diverse QCD based strong interactions involving other gluons and light quarks, the gluon density is the most capable of all QGP components to follow the evolution of the exploding/flowing matter closely, maintaining the chemical equilibrium abundance presented in Eq. (1). The formation time of QGP,  $\tau_{QGP} \simeq 0.2\text{--}0.8$  fm, is widely defined as the time needed for the gluon gas to reach initial absolute chemical equilibrium. Strangeness production by gluon fusion sets in at that time and is computed assuming chemical gluon equilibrium.

Hadronic particles seen in the final state can originate from different production processes; for example, strange hadrons may be formed

- during QGP hadronization, the reaction path of primary interest here;
- in initial high energy N–N interactions, the always present background in A–A collisions;

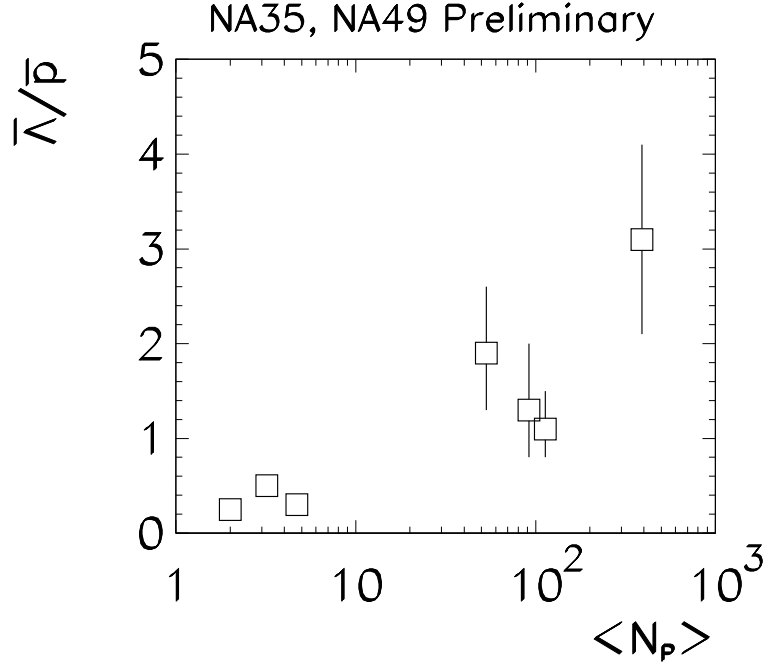


**Figure 1.** Preliminary experimental NA35/49 ratio  $\bar{\Lambda}/\bar{p}$  as function of number of participating baryons  $\langle N_p \rangle$  for different collision systems. From Ref. [10].

- in the reequilibrating and expanding hadron gas state following on the hadronization period, a process that could obscure the hadronic particle signatures of the QGP state;
- in secondary rescattering from spectator nuclear matter, a background we can minimize by an intelligent choice of triggers and collision partners

and should the QGP phase not be formed at all,

- during the various (equilibrium and non-equilibrium) stages of evolution of normal ‘hadronic gas’ (HG) matter, which is presumed to occur at sufficiently low collision energies.

It is thus important to focus our attention on the right experimental flavor signature, specifically here particle family, such as strange (anti)baryons, that is expected to be populated predominantly by hadronization of QGP — in [2] my concluding phrase says: *In the quark-plasma phase we expect a significant enhancement of  $\bar{\Lambda}$  production which will be most likely visible in the  $\bar{\Lambda}/\bar{p}$  relative rate.* This statement, explained in some detail in Eq. (2) below, is best compared to the current NA35/NA49 results which were recently presented [10], see figure 1. We see that when the number of participating nucleons  $\langle N_p \rangle > 30$ , this ratio is enhanced above the N–N ‘background’ where  $\langle N_p \rangle = 2$ , indeed there is a 10–30 fold enhancement. I note that the abundance of strange (anti)baryons will not be enhanced significantly in confined matter, even if overall strangeness production should increase driven by some yet unknown mechanisms which do not directly or indirectly invoke the collective dynamics present in QGP.

Comparable results are obtained for the ratios of cascades  $\Xi(ssq)$  with the lambdas  $\Lambda(sqg)$  by the NA49 [11] and by the more precise experiments WA85, WA94 [12], and WA97 [13]. A compilation of these results is shown in figure 2 as a ‘function’ of different experimental projectile and target combinations. These results were obtained with centrality triggers, assuring a qualitatively increasing number of participants from left to right in each of the three sections of figure 2. Dark squares are the recent Pb–Pb results as reported at the meeting [1] by the WA97 and NA49 collaborations. The central section in figure 2 addresses the enhancement in the ratio of strange antibaryons. Combined with the NA35/NA49,  $\bar{\Lambda}/\bar{p}$  results shown above in figure 1, these results imply a nearly 100 fold enhancement in the  $\bar{\Xi}/\bar{p}$  ratio over the N–N reaction background, a quite impressive result. Figure 2 also shows to the very left the production ratios arising in less precise measurements involving  $e^-e^+$  and  $p\bar{p}$  reactions. We will discuss the more precise ISR-AFS  $p$ - $p$  point further below.

We will now show quantitatively why this large enhancement in strange antibaryon yield from QGP phase could be anticipated so long ago. As discussed, the produced abundances of strange antibaryons are not controlled by (small) elementary N–N production cross sections, but by the quark chemistry occurring in the hadronization process, provided that the (anti)strange quark abundance is available. While the absolute particle yields depend on details of the hadronization process, relative yields of similar anti-baryon abundances are closely related to the available relative quark abundance:

$$\begin{aligned} \frac{\langle \bar{s}\bar{s}\bar{d} \rangle}{\langle \bar{u}\bar{s}\bar{d} \rangle} &\simeq \frac{\langle \bar{s}\bar{u}\bar{d} \rangle}{\langle \bar{u}\bar{u}\bar{d} \rangle} \simeq \frac{\langle \bar{s} \rangle}{\langle \bar{u} \rangle} \simeq \lambda_u \frac{\gamma_s}{\gamma_u} f_s \\ &\simeq 1.6 \frac{\bar{\Xi}^- \dots}{\bar{\Lambda} + \bar{\Sigma}^0 + \dots} \simeq 0.56 \frac{\bar{\Lambda} + \bar{\Sigma}^0 + \dots}{\bar{p} + \dots} \end{aligned} \quad (2)$$

In the first line in Eq. (2) we express the relative quark abundance in terms of thermal properties of the system. Here the values of the QGP parameters are known today; 20 years ago these have been just estimated. For the u-quark fugacity we have (see figure 3 below):  $\lambda_u \simeq \lambda_q \simeq 1.5$ – $1.6$ . Here  $\lambda_q$  is the  $(u, d)$ -light quark fugacity. The phase space occupancy ratio  $\gamma_s/\gamma_q \simeq 0.65$  as seen in different analysis of the SPS experiments. The relative size of the phase space volume of massive to massless quarks is (here  $K_2$  is a Bessel function):

$$f_s(m_s/T_f) = 0.5(m_s/T_f)^2 K_2(m_s/T_f) \simeq 0.65.$$

In the second line in Eq. (2) we relate the relative available quark abundance in the QGP to the relative abundance of produced strange antibaryons. This relationship applies if these particles are primarily produced in recombination processes, including in the available quark number the contribution from gluon fragmentation. The dots remind us that there are many hadronic resonances which can be populated in the hadronization process. These are taken into account with thermally weighted relative strength. After their fast hadronic decay they are contributing to the appropriate lowest stable hadronic state. We show on the hadronic scale stable  $\bar{\Sigma}^0$  state explicitly, since in all experiments it feeds into the  $\bar{\Lambda}$  yield, given its fast electromagnetic decay. This dilution effect is compensated by the factor 1.8 resp. its inverse, 0.56, which arise from the relative thermal abundance of two  $\bar{u}\bar{d}\bar{s}$  stable baryons (the more massive  $\bar{\Sigma}^0(I=1, I_3=0)$  is expected to be somewhat rarer than  $\bar{\Lambda}(I=0)$ ).

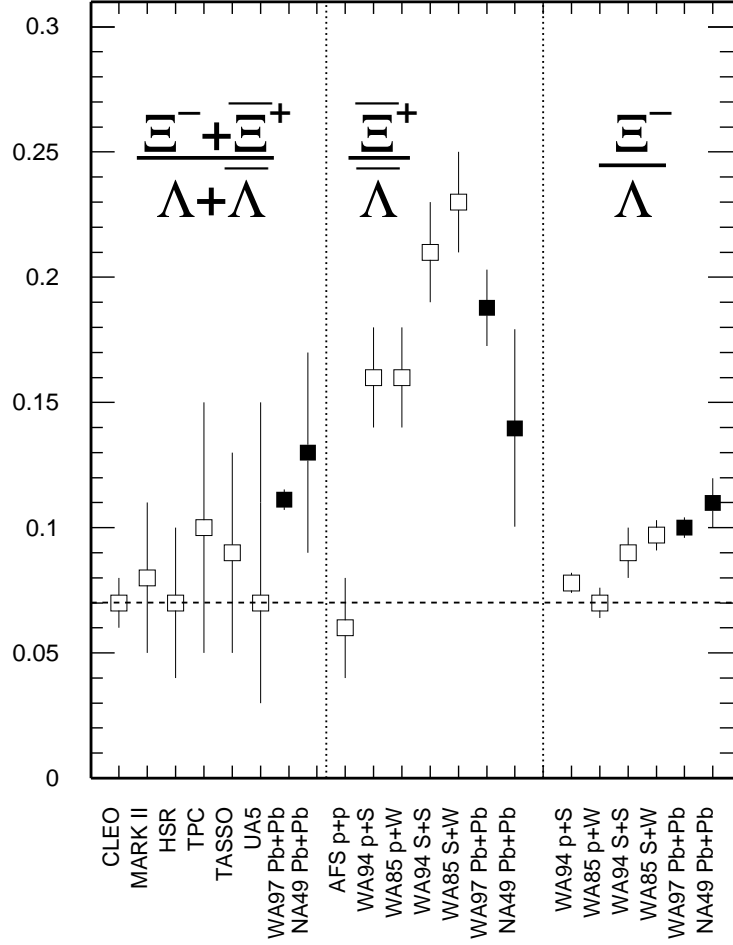


**Figure 2.** Ratios of cascades and lambdas and their antiparticles at fixed  $p_{\perp}$ , as ‘function’ of experiment name, ordered such that central particle multiplicity  $dN/dy|_{CM}$  increases from left to right. Nuclear collision results are for central rapidity  $\Delta y \simeq \pm 0.5$ ,  $SppS$ -UA5 high energy data ( $\sqrt{s} = 900, 546$  GeV) are for  $\Delta y \simeq \pm 2$ ,  $pp$ -ISR-AFS ( $\sqrt{s} = 31.5$  GeV) results are most central with  $\Delta y \simeq \pm 0.2$ . Dark squares: Pb–Pb 158 A GeV results as reported during the meeting are extrapolated to full  $p_{\perp}$ ; only statistical errors are shown. All other results have slightly varying high  $p_{\perp}$ -cuts with the lower limit between 1 and 1.4 GeV.

We find up to  $\mathcal{O}(20\%)$  precision, inserting in Eq.(2) the above discussed values of the statistical parameters:

$$3\bar{\Xi}/\bar{\Lambda} \simeq \bar{\Lambda}/\bar{p} \simeq 1. \quad (3)$$

This result is valid provided that there has been, prior to hadronization, enough time in the deconfined QGP phase to approach absolute strangeness chemical equilibrium. We see that, if deconfinement is achieved, multi-strange antibaryons will be produced in great abundance with a specific systematic pattern. Moreover, among final state particles the greatest signal to noise ratio has been expected for strange antibaryons, given the small background arising from N–N reactions.

Today there are of course much more elaborate theoretical models, yet this prediction of yesterday has withstood the test of time, for it relies on very simple ideas and principles. A quantitative comparison between strange antibaryon production by (a more elaborate) quark-chemistry mechanism and a string fragmentation model (tuned to describe the N–N interactions) shows that while quark-chemistry models are agreeing with experiment, the string model is not able to reproduce the strange antibaryon yields seen in the experiment [14].

### 1.3. From NN to AA collisions

Strange antibaryon production has been first explored in the early 1980's in central  $pp$ -interactions at CERN-ISR (Intersecting Storage Ring) by the AFS (Axial Field Spectrometer) collaboration [15], where the available N–N CM-energy was four times greater than it is now under study in nuclear collision experiments at SPS. The AFS-ISR results at  $\sqrt{s_{NN}} = 63$  GeV were determined in common fixed interval of transverse momentum  $1 < p_{\perp} < 2$  GeV:  $\bar{\Lambda}/\bar{p}|_{p_{\perp}} = 0.27 \pm 0.02$ ,  $\bar{\Xi}/\bar{\Lambda}|_{p_{\perp}} = 0.06 \pm 0.02$  (see figure 2), and at slightly higher  $p_{\perp}$ :  $\bar{\Omega}/\bar{\Xi}|_{p_{\perp}} < 0.15$  at 90% confidence. A few years later, a similar study was performed at yet much higher CM-energies at the CERN-SppS collider by the UA5 collaboration [16] (see figure 2), with relative yields remaining consistently small as given above.

In view of these emerging high energy  $pp$ - and  $p\bar{p}$ -experimental results, the abundance anomaly presented in Eq.(3) expected to be attained at much lower equivalent N–N collision energy seemed either impossible or, to others, implied that deconfinement would occur at energies above and beyond studied so far. But most importantly, there was a hadronic signature worth to look for experimentally in the nucleus-nucleus interactions: larger volumes of deconfined hadronic matter, when collided even at lower available energies, should produce particle abundances with unexpected features, qualitatively different from the ‘elementary’ N–N interactions.

The measurement of strange antibaryons in nuclear collisions could have in principle be carried out at the ISR-collider at CERN, where studies of inclusive  $\alpha$ – $\alpha$  reactions were already underway [17]. However the ISR, capable to deliver heavy ion beams up to 12–15 GeV CM-energy per nucleon, had been closed to make space for the construction of the Large Electron-Positron collider (LEP). Hence the experimental program proceeded at the SPS, which remained available, being used also as an injector for LEP. With nearly (by a factor  $\simeq 1.5$ ) the CM-energy of the ISR, the SPS could perform better at the time in certain tasks given the lengthening of the strange baryon weak interaction decay path by a factor  $\gamma \simeq 10$  in view of the center of momentum (CM) frame moving with rapidity  $y = \cosh \gamma \simeq 3$ . However, advances in silicon tracking make today a ‘small’ ISR-size collider a very attractive experimental tool suitable to continue the present day fixed target program.

In the past decade strongly interacting flavor probes of dense matter have been on the menu of the CERN-SPS experimental nuclear collision program. Several experiments, today referred to as NA57/WA97/WA94/WA85 and NA49/NA35, explored strange hadron production, including strange antibaryons, first in 200 A GeV Sulphur (S) beam interactions with laboratory stationary targets, including the symmetric S–S reactions, and Sulphur collisions with ‘heavy’ Silver (Ag), Gold (Au), Tungsten (W) or Lead (Pb) nuclei at 200 A GeV, and, more recently, moving on to the Pb–Pb collisions at 158 A GeV [18]. These results obtained at available energy of 8.6–9.2 GeV per participating nucleon will be soon complemented by strange antibaryon

data from 11 GeV Au-induced experiments carried out at the BNL-AGS.

Analysis of the global hadronic yields shows a great similarity in the behavior of dense matter at the AGS and SPS energies, despite 4 times higher available CM-energy at the SPS. The key difference between SPS and AGS is that hadronic particles produced at the lower AGS energies show features characteristic of confined matter chemical equilibration, such as is a finite non-negligible strange quark chemical potential. In principle, this is not in contradiction to possible formation of deconfined baryon rich quark matter at AGS energies, since hadronic abundance equilibration could be just a final state effect. Moreover, since for AGS energies it is expected that the specific entropy per baryon in confined and deconfined matter is very similar, there is to this date no clear evidence for, or against, QGP formation in the dense baryon rich matter fireballs made at AGS. The forthcoming measurement of strange antibaryon production should resolve this issue in the near future.

The measurement of strange antibaryons is not easy, and experiments need to be designed for the task as the relatively rarely produced strange antibaryons are literally buried in much more abundant mesons. Ways have to be designed to eliminate that background without losing the acceptance, which is required to observe mesons emerging from the self-analyzing decays such as  $\Xi^- \rightarrow \bar{\Lambda} + \pi^- \rightarrow N + \pi + \pi$ . An illustration of the experimental problems we experience is available when we look at the precision of the measurement of the ratio  $\bar{\Lambda}/\bar{p}$ . The preliminary NA49 result for Pb–Pb collisions [10], see figure 1, has a precision of 30%, so within 3 s.d. one could claim that the ratio is negligible, even though quite evidently in Pb–Pb collisions it is significantly greater than unity, defying the normal hadron production rules. One of the problems of measuring nucleons and anti-nucleons is that they do not self-analyze, which the weakly decaying strange baryons and antibaryons do. Moreover, the negatively charged antiprotons are at CERN energies produced less abundantly than  $K^-$ . Given the relativistic boost in fixed target experiments the proper identification of these particles poses a practical challenge.

#### 1.4. Strangeness enhancement

The validity of the strange particle signatures depends on the ability to produce high strangeness abundance in the dense matter. Considerable effort has therefore been devoted to the understanding of the kinetic mechanisms of flavor production. Kinetic theory studies of flavor production in QGP have shown that both the total strangeness yield, and thus the related emergence of an enhanced strange antibaryon yield [7, 19], are to be expected, and that the dominant strangeness production mechanism in hadronic matter is based on gluon induced reactions [5, 8, 9].

Whichever of the microscopic mechanisms one adopts for computation of the strange flavor production in the yet unknown form of high density nuclear matter that has been generated in relativistic nuclear collisions, one can identify the different factors controlling the yield in a rather model independent way. Consider two as yet unidentified constituent parts of centrally interacting nuclei,  $A$  and  $B$ , producing strangeness in individual collisions. The rate of production per unit of time and volume is given by

$$\left( \frac{dN_s}{dVdt} \right) = \langle \sigma_{AB}^s v_{AB} \rangle \rho_A \rho_B . \quad (4)$$

Since  $\rho = N/V$ , the specific strangeness yield per final state hadron is:

$$\frac{N_s}{n_h} \simeq \frac{N_A}{n_h} \cdot t \cdot \left\langle \frac{N_B}{V} \cdot \sigma_{AB}^s v_{AB} \right\rangle. \quad (5)$$

The relative particle abundance factor  $N_A/n_h$  is nearly independent of the internal structure in the dense matter fireball: the number of flavor producing particles  $A$ , which could be gluons and quarks, or could be pions, is a measure of the final hadron multiplicity  $n_h$ , except if new mechanisms are yet discovered for entropy production during the final state evolution. Similarly, the lifespan of the dense phase cannot depend decisively on the internal structure of the fireball, and thus as seen in Eq. (5), enhancement of strangeness production will be due primarily to the following two factors:

- (i) smaller effective volume  $V$  per particle (higher density), and/or
- (ii) enhanced microscopic cross section (e.g. dissolution of production thresholds).

Both these effects occur naturally in the deconfined phase. The second one has been postulated in order to generate strangeness enhancement in normal, confined hadronic matter. Within such an ad-hoc scheme the challenge for the inventor is then to demonstrate some other physical effect that would arise from such new and yet undiscovered confined hadronic matter phenomena. Perhaps equally relevant to the assessment of such proposals is the fact that one has to look for more than ‘strangeness enhancement’ with flavor observables, and in particular the (relative) yields of strange antibaryons originating in novel forms of confined matter should be also compared with the experimental data.

## 2. Ubi Sumus

### 2.1. Potential range of current experimental program

An illustration of the potential QGP coverage offered by the CERN-SPS and BNL-AGS accelerators is presented in figure 3, where i show the kinematic constraint between the statistical parameters temperature  $T$  and  $\lambda_q = e^{\mu_q/T}$ , the chemical light quark fugacity in an equilibrated QGP phase. To obtain these results [19], perturbative QCD equations of state (EoS) were evaluated in first order using  $\alpha_s = 0.6$ , and furthermore non-perturbative effects are taken into consideration by allowing for thermal quark and gluon masses:  $m^2 = m_0^2 + k(\alpha_s)T^2$ , where  $k = 2 = \text{Const.}$  was chosen. At this time it is not known how well such treatment of the QGP describes the transition to the confined HG phase. On the other hand, the two inter-dependent parameters  $c, \alpha_s$  as chosen yield properties of QGP at  $T \simeq 250$  MeV consistent with the observed nuclear collision results. Thus in that domain, assuming deconfinement, one can consider QGP EoS so determined to be adequate.

For each line shown in figure 3 the QGP energy per baryon  $E/b$  is set equal to the available kinematic energy content per baryon in the collision:

- (i) the dashed line bottom right is for the center of momentum (CM) per baryon energy  $E/b = 2.3 \text{ GeV}$ , corresponding to 11.2 GeV A projectile on fixed target Au–Au interactions at AGS;
- (ii) the dot-long-dashed line next to it is for  $E/b = 2.6 \text{ GeV}$ , corresponding to 14.6 GeV A Si–Au interactions at AGS;



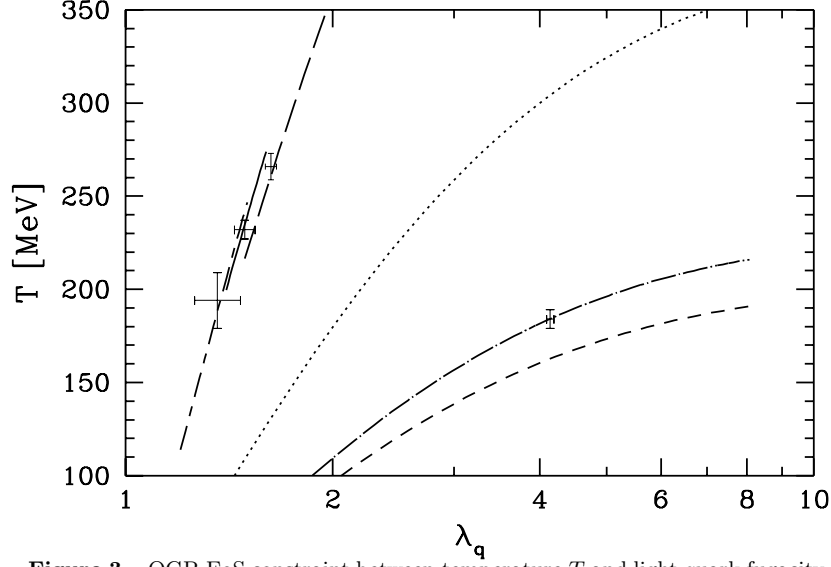


**Figure 3.** QGP-EoS constraint between temperature  $T$  and light quark fugacity  $\lambda_q$  for a given fireball energy content per baryon  $E/B$  appropriate for the AGS and SPS collision systems. Right to left: 2.3 (Au–Au), 2.6 (Si–Au), 4.3 (A–A), 8.6 (Pb–Pb), 8.8 (S–PB/W) and 9.6 (S–S) GeV. The Fermi( $u, d, s$ )/Bose( $G$ ) liquid EoS is used here to evaluate the QGP properties, with thermal particle masses  $m_i^2(T) = (m_i^0)^2 + 2T^2$ , and perturbative QCD interactions for gluons and  $u, d$  quarks with  $\alpha_s = 0.6$ . For theoretical details see [19].

- (iii) the dotted line in the middle is for  $E/b = 4.3$  GeV, corresponding to the low energy 40 A GeV limit of the SPS A–A runs scheduled for autumn 1999;
- (iv) the long dashed line is for the 158 A GeV Pb–Pb collisions at SPS, yielding  $E/b = 8.6$  GeV;
- (v) the solid line just next to it is for the 200 GeV asymmetric S–Au/Pb/W collisions, which give a slightly higher CM-energy content per nucleon,  $E/b = 8.8$  GeV, and
- (vi) the short-long dashed line is for the symmetric 200 GeV S–S collisions which in the CM frame yield is  $E/b = 9.6$  GeV.

Along these lines many properties of the system vary, such as entropy per baryon, pressure, baryon density. This variation corresponds to the variation in impact parameter and size of the colliding system: when the colliding nuclei are heaviest, there is less transparency, the baryon number is more compressed, the pressure of collision is higher, one reaches more extreme conditions moving to higher  $T$ ,  $\lambda_q$ . The same trend appears with increasing centrality of the collision, i.e., decreasing impact parameter.

The crosses in figure 3 represent the conditions reached in the respective collisions systems, based on chemical freeze-out analysis for  $\lambda_q$ , and the inverse slope of transverse energy particle spectra for  $T$ . The rationale for this estimate of the initial conditions in the dense QGP phase formed in the nuclear collision [19] is as follows:

- $T$ : The  $m_\perp$  inverse slope, rather than e.g.  $T_f$ , the freeze-out temperature, is employed, since one finds in schematic models that a qualitative relationship remains between the initial temperature and the high,  $m_\perp > 1.5$  GeV, inverse slopes. Intuitively this can be easily understood: when the transversely oriented flow of

matter sets in at high compression, it acquires thermal energy which is converted to collective kinetic energy. Along with energy conservation this roughly assures the relationship we need. However, both the nature of the transverse flow, and the way the inverse slope is determined introduces considerable model dependence. I thus believe that the inverse slope may be easily 10-15% different from the conditions at the onset of flow. On the other hand, the relative change in the inverse slope is much less model dependent as the collisions system is varied or the reaction energy changed. Thus the systematic change of the magnitude of the inverse slope with the size of the collision system shown in figure 3 is telling us that significantly higher initial temperatures are reached in Pb-Pb reactions compared to S-S reactions at the current SPS energies.

$\lambda_q$ : For isentropic (constant entropy, or equivalently constant entropy per baryon) expansion of the fireball to freeze-out condition the chemical fugacity undergoes negligible variation. This can be easily understood, since the specific entropy per baryon of massless quarks (massless on the scale of temperature) does not depend on a dimensioned parameter, thus it is just a function of  $\lambda_q$ , *i.e.*  $S/b = f(\lambda_q) = \text{Const.}$ , and hence  $\lambda_q = \text{Const.}$  for the isentropic expansion. A small correction at the level of a few percent is found due to the change of the quark-quark interaction strength, which varies logarithmically. Also, the strange quark mass is not negligible near freeze-out, but this strangeness effect is largely compensated by the entropy production associated with the formation of  $s\bar{s}$ -pairs.

As shown in figure 3, the SPS points cluster to the left and rise with the size of colliding system, from bottom to top: S-S, S-W/Pb, Pb-Pb. The AGS result shown to the right in the figure for Si-Au case, falls in principle into a different category, since the strange chemical potential measured in the reaction does not vanish, yet it falls onto the QGP constraint line.

Inspecting the SPS results we see that a variation in the atomic number  $A$  of the colliding nuclei, which can be nearly equivalent to a choice of different centrality of the reaction, will introduce another data point along these three lines shown. In order to fill the big gap in-between SPS and AGS, a 40 A GeV run is scheduled for 1999 at the SPS. Thus within the forthcoming 18 months we will be able to bridge (see dotted line in figure 3) the energy gap between CERN and AGS data. Such a more complete coverage of the statistical parameter range is the primary physics motivation to reduce SPS beam energy.

## 2.2. Experimental progress

Do any of the recent strangeness results suggest the presence of new physics, or can we deal with these data on the basis of known phenomena, without invoking the local color deconfinement? A clear answer to this question is, in my opinion not available yet, but a number of highly noteworthy experimental and theoretical results are pointing in the direction of QGP, we have here discussed in depth the enhancement of antibaryons which has been observed at CERN-SPS in the way it has been predicted. Thus, if there was other convincing supporting evidence, *e.g.* from dilepton or direct photon observables, this conclusion could probably be reached today. Moreover, the widely discussed topic of charmonium suppression is not helping here, since there seems to be a great difference in the physics result comparing S and Pb induced reactions, which we do not really notice in the strange particle abundances.

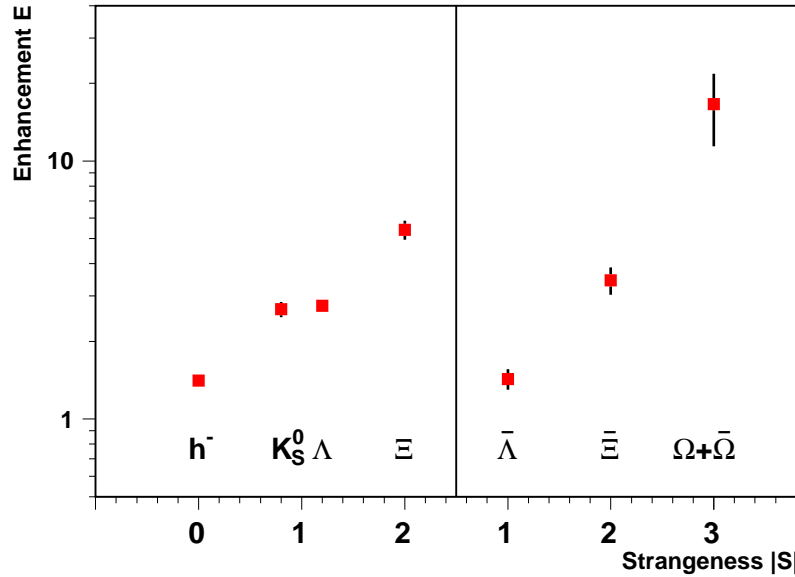


**Figure 4.** Strangeness enhancement versus strangeness, WA97 collaboration [21].

In addition, the experimental strangeness results have not yet been analyzed in full. The sheer abundance of experimental hadronic particle data is very large, and it takes considerable effort to obtain precise hadronic abundances and spectra. For example, in the past 18 months, the WA97 collaboration has analyzed only a fraction of their data tapes obtained in the autumn 1996 run involving Pb–Pb 158 A GeV collisions at CERN-SPS [13]: their analysis is reaching 40% for multi-strange (anti) baryons  $\Xi$ ,  $\bar{\Xi}$ ,  $\Omega$ ,  $\bar{\Omega}$ , but barely scratched the analysis of  $\Lambda$  and  $\bar{\Lambda}$  yields. The NA49 collaboration continues to review their initial 1995 and 1996  $\bar{\Lambda}$  and  $\Lambda$  results and has presently announced progress in understanding the impact of the cascading decays from  $\Xi$  and  $\bar{\Xi}$ , which populate the central yields of  $\Lambda$  and  $\bar{\Lambda}$  particularly strongly, given the large size of the NA49-TPC set-up [20].

Returning to the possibility of QGP formation, we note the strangeness enhancement effect has been studied now in considerable detail, and there is a well reported evidence assembled over the past 10 years in all the pertinent BNL and CERN experiments. Without presenting it here in every detail, I note that in several slightly varying definitions of the word, this enhancement is reported to be a factor  $2.5 \pm 0.5$ , as it has been predicted if QGP is formed. Moreover, this enhancement is consistently rising with the multi-strangeness of hadrons. This is most easily seen in the recent results presented by R. Lietawa for the WA97 collaboration [21], see figure 4, where the different enhancement factors obtained in the same experiment (same trigger centrality, same data analysis method) are shown. We see in figure 4 the enhancement over the expected yield, with the basis provided by the N–A reactions measured in the same experimental setup. The extrapolation from A–A reactions to N–A reactions is made implementing a linear scaling of particle yield with the number of participant nucleons, a point carefully documented by the WA97 collaboration in terms of the trigger dependence of particle yields. This part of the analysis shows that the A-scaling of strange particle production is assured, when the number of

participants exceeds about 100. Thus, somewhere on the way from a few participants (N–A interactions) to triggered central A–A interactions, the yield has to rise in a nonlinear fashion with the participant number and the strangeness enhancement here presented arises. Note that in figure 4 the particle abundance enhancement increases significantly as we consider the production of particles, which require assembly of constituents not brought into the reaction by colliding nuclei.

Figure 4 also shows enhancement of negative hadrons (factor 1.5) and single-strange hadrons (factor  $\simeq 2.8$  for  $K_s$ ,  $\Lambda$  and factor  $\simeq 1.5$  for  $\bar{\Lambda}$ ). Thus the entropy and strangeness yield are both increasing in parallel in Pb–Pb reactions, again as would be expected if melting of the color bonds of quarks occurs for both light and strange quarks. But the crucial point seen in figure 4 is that the yield increase of multi-strange hadrons is in general much stronger, reaching a factor of 4.5 for  $\Xi$  and above 10 for the triple strange Omegas. This effect is the anticipated and specific signal of formation and breakup of a deconfined space-time region, and has so far eluded models that rely on confined matter. In conclusion, we see a systematic pattern of strange particle enhancement in figure 4 and note that at present the only model capable to reproduce this result is QGP fragmentation-recombination hadronization.

The current status regarding relative abundances at central rapidity of cascades and lambdas and their antiparticles is displayed in figure 2, while the relative yields of anti-lambdas and antiprotons are shown in figure 1. In figure 2, the dark squares are the recent Pb–Pb results as reported at the meeting [11, 13]. These new results refer to the full range of  $p_\perp \in (0, \infty)$ , while the earlier data (e.g., of collaborations WA85 and WA94) refer to ratios for  $p_\perp > 1.2$  GeV. This explains in part the reduction in value of some of the ratios shown. The other effect contributing to the reduction of  $\Xi/\bar{\Lambda}$ -ratio is the Coulomb effect in Pb–Pb collisions, which has noticeable impact on relative strange particle yields from deconfined matter. Note also the  $pp$  and  $ee$  interaction results in figure 2, which offer comparison with the backgrounds from elementary interactions. Current WA97 data offer for the first time solid proof (by many standard deviations) of the enhancement by a factor of 3 for  $\Xi/\bar{\Lambda}$ , since both the results from ISR-AFS- $pp$  interactions and the WA97 results from Pb–Pb interactions are sufficiently precise. This enhancement is even more remarkable, considering that the available energy in the Pb–Pb collisions has been four times smaller than the energy available at the ISR N–N interactions.

The AGS experiments were initially focused on other ‘strange’ issues, and in particular many resources have been vested to seek strange nuclear matter. Only recently the study of strange antibaryons as a possible signature of the deconfined state, has commenced, for there are strong indications, e.g. in the E802/E859/E866 experiment series, that the yield of  $\bar{\Lambda}$  exceeds the yield of  $\bar{p}$  at AGS energies. We have seen at the meeting, that there is a continued and considerable effort devoted in experiments E917 [22] and E895 [23] to measure systematically strange particle yields as a function of energy, up to 11 A GeV. It is an interesting race against time, for the completion and availability of RHIC is likely to overpower AGS experimental efforts in a not too distant future.

### 2.3. Hadrons from QGP

If quark-gluon plasma is produced in nuclear collisions, a major theoretical challenge is the understanding of the hadronization process. In principle, production and emission of particles can occur throughout the evolution of the dense matter fireball. However, it

has been generally assumed that the bulk of particles is produced in the final moments of evolution when the temperature of dense matter sinks below the deconfinement condition. The cooling of matter is not necessarily a result of energy radiation, generally it is believed to be primarily due to the transfer of local thermal energy to the collective flow of matter. Such a collective expansion process can be nearly entropy conserving, since for  $S \propto VT^3$  [or better  $S \propto \int d^3x T^3(x)$ ] the increase in system size is compensated by a corresponding decrease in  $T$ .

To proceed, we need to clarify the understanding of the different local chemical equilibria introduced earlier [7]. We distinguish two cases for their different reaction time scales. The slower *absolute* chemical equilibration requires that the particles produced build-up to fill the available phase space; for the faster, *relative* chemical equilibrium, a weaker requirement suffices, namely the redistribution of some property (here quark flavor) among different carriers (particles) according to the relative phase space size. A sample of alternative evolution scenarios that could be responsible for the production of the final state hadrons includes:

- (i) If the hadronization temperature is low (say below 145 MeV), it can be safely assumed that there will be little, if any, subsequent change in the hadron abundances. Chemical equilibrium, in which quark and gluon abundances are fixed to the Stefan-Boltzmann limit should not be presumed, neither for the source of the hadrons, nor for the hadron yields after hadronization. In this case of ‘low’ hadron formation temperature, hadronization is also the chemical freeze-out, and the study of the chemical freeze-out conditions can reveal valuable information about the QGP phase. This seems to be the situation we encounter at SPS energies.
- (ii) If hadron production from the deconfined phase were to occur at conditions that are more dense (in terms of baryon density, or particle density in general, synonymous with higher temperature), chemical re-equilibration among confined final state hadrons should occur, erasing the eventual particle abundance signature of the primordial QGP phase; this is possibly the situation at AGS energies.
- (iii) The possibility of explosive and continuous disintegration cannot be ruled out at present. In this scenario, beginning at high temperatures QGP phase decays successively by emission of free-flowing particles. In that conditions we can use hadronic particles again to establish the properties of the plasma phase. For isentropic fireball evolution, which in the QGP phase means that the quark fugacities are unchanged, a consistent determination of chemical parameters is also possible in this case, using final state hadron abundances.

Since QGP chemical properties are rather characteristic, e.g., the strange quark chemical potential is nearly zero in the deconfined phase, analysis of hadron abundances can tell us if a re-equilibration process has been occurring. The experimental data at SPS energies favors, as I see it, a scenario in which no chemical re-equilibration did occur after hadronization. This means that hadronization/chemical freeze-out are the same process.

Even if re-equilibration were to occur, dynamical calculations show [7] that it is highly unlikely that the number of strange quark pairs changes significantly once, speaking in relative terms, the low density post-freeze-out phase has been established. One can thus infer strangeness abundance and phase space occupancy conditions present at QGP hadronization rather precisely from the final state hadron abundances.

To derive QGP strangeness occupancy we need to consider that the phase space density of strangeness in QGP and HG phases is different. Therefore, the phase space populations must be appropriately adjusted to infer from the observed final state yield of strange quarks per baryon number the conditions in the earlier QGP phase. Moreover, several chemical analysis of the data, which reported that the strangeness phase space was saturated up to about 70% in the final hadronic phase, have indeed been reporting the *ratio of strange to non-strange* phase-space saturation. The non-strange quark occupancy is at 150–200% of the equilibrium, as is noted by the excess of mesons (excess entropy). Allowing for this effect we see that the strangeness phase space is overpopulated in the HG phase, but not in QGP. Without invoking QGP formation it appears as if the chemical strangeness equilibrium were approached from above, a situation difficult to justify. The parallel overpopulation of the light quark phase space is also in contradiction with the HG phase hypothesis, but is also expected to arise if QGP is formed: the glue degree of freedom must fragment into quarks in the hadronization process in order to preserve the enhanced entropy originating in the melted color bonds.

As particles emerge from the QGP hadronization, not only their abundance but also their spectra will be unusual. Indeed, some bold conclusions about the origin of the strange antibaryons can be inferred from the remarkable experimental fact that the transverse mass spectra are so similar for particle-antiparticle pairs (e.g.,  $\bar{\Lambda}$ – $\Lambda$ ,  $\Xi$ – $\bar{\Xi}$ ), as seen in results of the precise measurements made by experiments NA49 and WA85/WA94/WA97:

- (i) The thermal equilibrium in heavy ion collisions is relatively well established; for very different spectra should be arising from hadron based reactions (for strange baryons associate production  $N+N \rightarrow \Lambda+K$ , direct pair-like production for antibaryons) as is seen in many microscopic models simulating the nuclear collision process.
- (ii) The exponential shape of the  $m_{\perp}$ -spectra with a common inverse slope implies further that these particle pairs, or the building blocks from which they are made in a coalescence picture, had reached well thermalized condition.
- (iii) The shape identity of the transverse mass spectra of these pairs implies that they have either been dragged in the same manner by the flowing hadronic matter, or that they were emitted by a flowing surface source and reached the detector without much further interaction.
- (iv) Since the drag forces of the flowing matter can be expected to be greatly different for the  $\bar{\Lambda}$ – $\Lambda$  particle pair, and since it can be today subsumed that there is considerable transverse flow with  $|\vec{v}_{\perp}| \propto 0.5 c$  at the time of particle freeze-out, one is driven to the conclusion that these strange baryons and antibaryons were not ‘dragged’ along in confined matter, and thus must have been formed in coalescence of flowing, thermally equilibrated deconfined matter.

We see that not only the yields of strange (anti)baryons, but also the details of their spectra are relevant and will contribute significant information about the production mechanism and the possibly deconfined nature of the hadron source.

#### 2.4. Theoretical directions

There are many theorists working on flavor observables and the theoretical tools are continuously improved. A short list of ongoing activities includes:

- (i) Production of heavy (strange, charm) flavor:
  - (a) in (thermal) QGP;
  - (b) in parton and string models;
  - (c) confined/deconfined state comparisons.
- (ii) Evolution of hadronic matter and formation of hadrons in final state:
  - (a) collective flow of dense matter,
  - (b) hadronization,
  - (c) hadrochemistry,
  - (d) approach to chemical equilibrium.
- (iii) Analysis of experimental results:
  - (a)  $m_{\perp}$ ,  $y$ -spectra;
  - (b) particle abundances;
  - (c) HBT correlation analysis.

As indicated above in (i), there are several distinct classes of theoretical approaches to strangeness production in high energy nuclear collisions. A simple classification arises dividing the models into progressively more microscopic approaches:

*local thermal and chemical equilibrium models,*  
*local thermal equilibrium and kinetic description of chemical reactions,*  
*fully kinetic (microscopic) reaction models.*

Within the local kinetic (temperature) equilibrium description, allowance must be made for associated spatial and temporal distribution of temperature (energy density), and chemical potentials, and also the collective flow velocity. Among the local equilibrium descriptions, I distinguish between those based on

*hadronic gas constituents*            and those based on  
*quark-gluon matter.*

In both cases there are different levels of treatment of chemical equilibration:

*assume relative equilibrium, but not ‘absolute’ chemical equilibrium,*  
*treat only heavy (strange) quarks using kinetic theory,*  
*use kinetic theory for all chemical processes.*

When full chemical kinetic theory is employed, we indeed have gone half way to microscopic models of collision dynamics, which do not assume thermalization of constituents. But even in fully microscopic descriptions there are several distinct classes, we distinguish two primary approaches:

*hadronic cascades* involving *reactions between individual hadrons* and  
*quark cascades*, which may be further differentiated as  
*color string models* and  
*parton (cascade) models.*

This short classification of the theoretical approaches is in no way complete, as practically all types of hybrid models have also been proposed. For example, models which combine a smooth transition from confined to deconfined structure, or which address kinetic theory of heavy quarks in the thermal background of light quarks and gluons.

Why do we need so many different models? Nobody doubts that microscopic models are superior to statistical models (and hence is this what we all should be doing?), but some of us also realize that, in practice, microscopic approaches suffer critically from the need to understand and be able to model all relevant and accessible reaction mechanisms, including the novel phenomena that are yet to be discovered. Thus practice calls for compromise solutions, in which some aspects are considered to be sufficiently precisely described in a simpler (statistical) manner. Moreover, the degree to which the reaction is treated as a quantum mechanical process, as compared to classical two particle cascades, is not understood in principle. In fact, even if we had much greater computing power available allowing us to compute within fundamental theoretical approaches such as lattice-QCD [24], we would not know how to treat the dynamics of the collision, the transition from quantum to classical dynamics, the non-equilibrium aspects and many other issues. So the multitude of approaches really reflects on the exploratory character of the research we are engaged in.

Each model has its pros and cons: microscopic models cannot be used to interpret results without fine tuning the various implicit and explicit reactions. The thermal models suffer not only from the perception that kinetic equilibrium is introduced *deus ex machina*, without proper understanding of the dynamics and time scales involved. However, the reaction dynamics in local equilibrium models are usually relatively simple and often allow one to come to model-independent conclusions about suitably defined observables. However, before using a statistical description we must scrupulously test which quantities can be treated by near-equilibrium methods. This often requires the tools of a microscopic model. So both approaches are indeed complementary.

### 3. Quo Imus: Where are we going?

Quark-gluon plasma is, by the meaning of these words, a thermally equilibrated state consisting of mobile, color charged quarks and gluons. There is no requirement for chemical equilibration, in which quark and gluon abundances are fixed to the Stefan-Boltzmann limit. In laboratory experiments only a very short-lived QGP phase can be established, and thus by the nature of the circumstance we should expect, if at all, a deconfined state in a chemical non-equilibrium. Moreover, entropy and total strangeness excesses are the global observables of deconfinement. There is the fundamental issue if thermal equilibrium can be attained in the short time available. This is a very controversial question, which we would like to address by inspection of experimental results, which seem to be strongly in favor.

The chemical analysis of (mostly strange) hadrons produced in high energy nuclear reactions offers opportunity for:

- (i) a precise determination of the overall strangeness yield;
- (ii) determination, if for some rarely produced particles the chemical equilibrium is approached from below or above, the latter case pointing to deconfinement;
- (iii) an assessment, if strangeness excess is accompanied by entropy excess as would be expected for deconfined source at hadronization.

An important aspect here is that the specific yield of strangeness produced seems to fall rapidly with decreasing available collision energy, or increasing reaction volume (or both). The lowest yield seems to occur in the 158 A GeV Pb–Pb reactions, where a detailed study of the phase space occupancy suggests specific abundance at the



level of  $\bar{s}/b = 0.6\text{--}0.7$ . Same type of analysis yields nearly 50% higher abundance at the level of  $\bar{s}/b = 0.9\text{--}1.0$  for S-W/Au/Pb 200 A GeV collisions. Yet higher yields are suggested by S-S 200 A GeV results, though details are obscured by the strong longitudinal flow present in this light, yet smaller system — the available energy is here still higher since the collision is symmetric.

- Could it be that this rapid rise in strangeness yield with collision energy occurs since the current SPS experiments occur just at the threshold to deconfinement? Alternatively:
- Is it possible that this rapid change in strangeness yield is an intricate effect of the dynamics of highly compressed dense quark matter arising in particular from differences in the lifespan of the high temperature deconfined phase?

We need to clarify this important issue.

Detailed interpretation of experimental strange flavor flow results requires almost always an understanding of the general reaction dynamics expressed by baryon and meson spectra. These measurements in fact give us an idea about the stopping of energy and baryon number in the central fireball and the entropy (particle multiplicity) yield per participant. This study can be combined with a comprehensive analysis of the abundance freeze-out conditions of strange hadrons. In such an analysis chemical non-equilibrium features for both strange and non-strange particle production need to be included. In that way one obtains a snap-shot of the dense matter fireball, taken when strange hadrons stop changing in number, i.e., at the chemical freeze-out.

Beyond the chemical properties, the local surface rest-frame temperature  $T$  and local collective flow velocity  $\vec{v}_c$  characterize the momentum space distribution of particles emerging and can be studied in such final state analysis. However, particles of similar mass and cross section with the background (compatible particles) experience similar drag forces arising from the local flow of matter and hence the ratio of their abundances in some limited region of phase space, for not too small momenta, is expected to remain similarly altered by  $\vec{v}_c$ . While the surface vector flow  $\vec{v}_c$  is a priori largely unknown, one simple hypothesis is radial explosion with the transverse to collision axis surface velocity reaching the ‘sound’ velocity of massless matter,  $c/\sqrt{3}$ . This discussion shows that the theoretical analysis, even in the statistical approach is as tedious as is the experimental data analysis. In conclusion, the theoretical study of the great wealth of experimental hadronic data is not easy, but there has been considerable progress made in recent years, with results becoming more reliable and consistent between the different groups and strategies of approach.

The information we extract tells us, in principle, only about the momentary physical properties of the dense fireball. However, even such a snap-shot taken at the end of the chemical evolution contains clear information about earliest moments of the collision: the total yield of heavy flavor is primarily determined in the initial stages of the collision. Since it is mainly produced by chemically equilibrated gluons, in particular charm, and to a lesser degree also strangeness yield is determined by the initial temperature. The situation is best understood inspecting figure 5, where the differential rate of production of flavor,  $f = q, s, c$ , is shown as a function of temperature, for the dominant gluon fusion process. The interaction strength of the perturbative QCD is gauged at the decay of the  $Z_0$  particle, and is not a free parameter in this calculation. However, for strangeness (but not for charm) the uncertainty in  $m_s(1\text{ GeV})$  translates into an uncertainty of 25% in the production rate shown. We see in figure 5 [25], that the expected rate of charm production at  $T = 500\text{ MeV}$  is

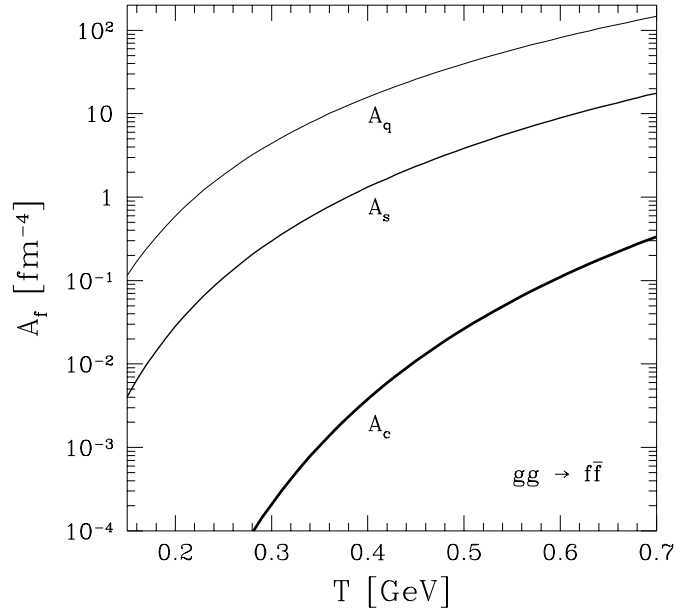


**Figure 5.** Invariant thermal rate  $A_f$  per unit time and volume as function of temperature  $T$  for production of quark pairs in gluon fusion processes  $gg \rightarrow f\bar{f}$ , where  $f$  is either the light quark  $q = u, d$  flavor (thin line,  $m_q(1 \text{ GeV}) = 10 \text{ MeV}$ ), or strange  $s$  ( $m_s(1 \text{ GeV}) = 200 \text{ MeV}$ ) or charm  $c$  quark flavor (thick line,  $m_c(1 \text{ GeV}) = 1.5 \text{ GeV}$ ); after [25].

nearly equal to the rate of strangeness production at  $T = 200 \text{ MeV}$ : specifically

$$A_c(500 \text{ MeV}) \simeq 0.03/\text{fm}^4 \simeq A_s(200 \text{ MeV}).$$

This implies that the total yield of charm at RHIC will be as abundant as that of strangeness at AGS. However, per hadronic particle produced it will be 16 times smaller, considering that the entropy content scales with third power of  $T$ .

We conclude that open charm is more than strangeness a ‘deeply penetrating’ probe of the early QGP conditions, much akin to dilepton and direct photon signals. These electromagnetic signals are, unlike heavy flavor, ‘deeply hidden’ in the general reaction background, and indeed even the decay products of open charm provide here considerable background. However, this can be a blessing: the reported excess of the dilepton yield below the  $J/\Psi$  resonance has been shown at this meeting to be consistent with the decay of open charm mesons [26], a very tantalizing suggestion that is likely to stimulate the effort for direct measurements of charmed meson decays, in principle possible in the NA57 experiment at SPS (successor to WA97), and we are looking forward to copious appearance of this flavor observable at RHIC energies, and its use as a deeply penetrating diagnostic tool.

We thus have, in the absolute yields of strangeness and charm, a measure of the initial stage of the collision and in the relative hadron yields a snap-shot picture of the freeze-out conditions. Can this information illuminate the issue of deconfinement? Definitely so, if we are able also to obtain many different snap-shots of the chemical freeze-out, varying energy of colliding nuclei, and the participating amount of matter.

Let me close with a few general remarks: I am not able to look further than the next two years into the future, given the phase transition the community is undergoing

presently: the exploratory fixed target programs at SPS and AGS are coming to an end while the dedicated measurements of the properties of deconfined phase are likely to begin at RHIC, where in fact the physics is completely unknown. However, the discussion we have presented provides for a clear shopping list, which we will need to fill in next two years. My personal experimental and theoretical priorities are as follows:

### Experiment

- (i) Complete analysis of SPS-158 A GeV, with the aim of presenting both particle spectra and precise relative hadronic/strange particle yields;
- (ii) Determine the yield of strange antibaryons at the AGS Au-beam.
- (iii) Obtain strange particle yields, and spectra, at the energy intermediate between AGS and maximum available at SPS, and compare with the lower/higher energy results in comparable conditions.
- (iv) Ramp the energy of the SPS up to check if strangeness yield rises even with a (small) energy increase. Vary the size of projectile/target combination (e.g. using Ag–Ag collisions or/and trigger condition on heavy projectile/target combination) to see how energy and reaction volume combine to determine the overall strangeness yield.
- (v) Obtain first results on reaction mechanisms and strangeness production (Kaons) at the 12 times higher energies becoming available at RHIC.
- (vi) In view of the likely phase-out of experimental research programs at AGS and SPS, and the likely occurrence of the deconfinement transition below the lower RHIC energy limit (4 times the current SPS-CM-available energy) commence development of a nuclear intersecting beam collider ranging the deconfinement transition region.

### Theory

- (i) Complete development of consistent analysis programs of the experimental data based on competing reaction mechanisms (confinement/deconfinement) and theoretical approaches (thermal/kinetic/parton).
- (ii) Refine the understanding of the hadronization mechanisms of quark-gluon plasma and the production of strange hadrons at phase transition conditions.
- (iii) Develop the equations of state of hot and dense thermal matter in confined and deconfined conditions without assumptions about chemical equilibrium.
- (iv) Continue progressing towards an understanding of QCD-vacuum structure and properties of the phase transition at finite baryon density.

I am looking forward to our next meeting to be held in July 2000. All welcome to **Strangeness 2000–USA!**

### Acknowledgments

I would like to thank U. Heinz, J. Letessier, and E. Quercigh for the careful reading and valuable comments about the contents of this manuscript, and collaborations

NA35/NA49 and WA97 for the permission to use their figures. This work was supported by a grant from the U.S. Department of Energy, DE-FG03-95ER40937.

## References

- [1] Proceedings of the International Conference: *Strangeness in Quark Matter 1998*, held in Padova, July 20–24, 1998, to appear in *J. Phys. G* (1999), M. Morando et al., Eds.
- [2] J. Rafelski, pp 282–324, GSI Report 81-6, Darmstadt, May 1981; Proceedings of the Workshop on *Future Relativistic Heavy Ion Experiments*, held at GSI, Darmstadt, Germany, October 7–10, 1980, R. Bock and R. Stock, Eds., (see in particular section 6, pp 316–320); see also:  
J. Rafelski, pp 619–632 in *New Flavor and Hadron Spectroscopy*, Ed. J. Tran Thanh Van (Editions Frontiers 1981), Proceedings of XVIth Rencontre de Moriond – Second Session, Les Arcs, March 21–27, 1981;  
J. Rafelski, *Nucl. Physics A* **374**, 489c (1982) — Proceedings of ICHEPNC held 6–10 July 1981 in Versailles, France.
- [3] J. Rafelski and R. Hagedorn, in: *Statistical Mechanics of Quarks and Hadrons*, H. Satz, Ed., North Holland, (Amsterdam 1981) p. 253.
- [4] T.S. Biro and J. Zimanyi, *Phys. Lett. B* **113**, 6 (1982); *Nucl. Phys. A* **395**, 525 (1983).
- [5] J. Rafelski and B. Müller, *Phys. Rev. Lett* **48**, 1066 (1982); **56**, 2334E (1986); J. Rafelski, *Phys. Rep.* **88**, 331 (1982).
- [6] J. Rafelski, *Nucl. Phys. A* **418**, 215 (1984).
- [7] P. Koch, B. Müller and J. Rafelski, *Phys. Rep.* **142**, 167 (1986).
- [8] N. Bilić, J. Cleymans, I. Dadić and D. Hislop, *Phys. Rev. C* **52**, 401 (1995).
- [9] J. Letessier, J. Rafelski, and A. Tounsi, *Phys. Lett. B* **389**, 586 (1996).
- [10] D. Röhrig, for the NA49 Collaboration, “Recent results from NA49 experiment on Pb–Pb collisions at 158 GeV per nucleon”, Jerusalem 1997, to appear in proceedings; NA49 note 145, available at: <http://na49info.cern.ch/cgi-bin/wwwd-util/NA49/NOTE?145>.
- [11] Frank Gabler, for the NA49 Collaboration, in this volume.
- [12] David Evans, for the WA85 and the WA94 Collaborations, in this volume.
- [13] R. Caliendo, for the WA97 collaboration, in this volume, and private communications.
- [14] P. Csizmadia, P. Levai, S.E. Vance, T.S. Biro, W. Guylassy, and J. Zimányi, in this volume.
- [15] T. Åkesson et al., AFS-collaboration, *Nucl. Phys. B* **246**, 1 (1984).
- [16] R.E. Ansorge et al., UA5-collaboration, *Nucl. Phys. B* **328**, 36 (1989).
- [17] T. Åkesson et al., AFS-collaboration, *Phys. Rev. Lett.* **55**, 2535 (1985).
- [18] J.B. Kinson, in this volume.
- [19] J. Rafelski, J. Letessier and A. Tounsi, *Acta Phys. Pol. B* **27**, 1035 (1996), and references therein.
- [20] Spiros Margetis, for the WA49 Collaboration, in this volume, and personal communication.
- [21] R. Lietawa for the WA97 Collaboration, in this volume.
- [22] R. Ganz, for the E917 Collaboration, in this volume.
- [23] P. Chung, for the E895 Collaboration, in this volume.
- [24] E. Laermann, *Nucl. Phys. A* **610**, 1c (1996).
- [25] J. Letessier and J. Rafelski, “Charmed Particle Signatures of Deconfinement”, in preparation.
- [26] E. Scomparin, for the NA50 Collaboration, in this volume.